

Direct observation of vibrational coherence in bacterial reaction centers using femtosecond absorption spectroscopy

(photosynthesis/charge separation/mutant)

MARTEN H. VOS^{†‡}, JEAN-CHRISTOPHE LAMBRY[†], STEVEN J. ROBLES[§], DOUGLAS C. YOVAN[§], JACQUES BRETON[‡], AND JEAN-LOUIS MARTIN[†]

[†]Laboratoire d'Optique Appliquée, Institut National de la Santé et de la Recherche Médicale Unité 275, Ecole Polytechnique-Ecole Nationale Supérieure de Techniques Avancées, 91120 Palaiseau, France; [‡]Service de Biophysique, Département de Biologie, Centre d'Etudes Nucleaires de Saclay, 91191 Gif-sur-Yvette Cedex, France; and [§]Department of Chemistry, Massachusetts Institute of Technology, Cambridge, MA 02139

Communicated by Robin M. Hochstrasser, June 17, 1991 (received for review April 12, 1991)

ABSTRACT It is shown that vibrational coherence modulates the femtosecond kinetics of stimulated emission and absorption of reaction centers of purple bacteria. In the D_{LL} mutant of *Rhodobacter capsulatus*, which lacks the bacteriopheophytin electron acceptor, oscillations with periods of ≈ 500 fs and possibly also of ≈ 2 ps were observed, which are associated with formation of the excited state. The kinetics, which reflect primary processes in *Rhodobacter sphaeroides* R-26, were modulated by oscillations with a period of ≈ 700 fs at 796 nm and ≈ 2 ps at 930 nm. In the latter case, at 930 nm, where the stimulated emission of the excited state, P*, is probed, oscillations could only be resolved when a sufficiently narrow (10 nm) and concomitantly long pump pulse was used. This may indicate that the potential energy surface of the excited state is anharmonic or that low-frequency oscillations are masked when higher frequency modes are also coherently excited, or both. The possibility is discussed that the primary charge separation may be a coherent and adiabatic process coupled to low-frequency vibrational modes.

The quantum efficiency of the initial charge-separation process in the reaction center of photosynthetic bacteria is near unity because of the combination of the extreme rapidity of forward electron transfer and the low probability of back reaction. In conventional electron-transfer theory (1, 2), it is assumed that vibrational relaxation takes place on a time scale faster than electron transfer and that electron transfer is essentially nonadiabatic. It may be questioned whether these assumptions are justified for the ultrafast initial reactions taking place in the bacterial reaction center. In particular, electron transfer from an excited state that is not completely vibrationally relaxed (3) may be at the origin of the high quantum yield of charge separation. In this case, vibrational coherence of modes coupled to electron transfer is not necessarily lost on the time scale of the reaction. Recently, theoretical studies have appeared in which it has indeed been suggested that vibrational coherence or coherence in the electronic coupling, or both, play a role in primary electron transfer (4–7).

If the vibrational relaxation takes place on a time scale that is not significantly faster than electron transfer, low-frequency (<100 cm⁻¹) vibrations may interfere with the charge-separation reaction. When such vibrations are coherent, oscillations may in principle be observed in the optical transients of the involved electronic state(s). Here we report the observation of coherent processes associated with the excited state in the photosynthetic reaction center.

The reaction center of purple bacteria, which are used in this study, normally contains four bacteriochlorophylls [two

of which display strong dimeric interaction and are designated P (for “special pair”) and two of which, B_L and B_M, are more monomer-like], two bacteriopheophytins (H_L and H_M), and two quinones (Q_A and Q_B) bound to the protein subunits L and M (8, 9). The lower-exciton excited state of the dimer, P*, is the precursor of electron transport; the charge-separated state P⁺H_L⁻ is formed in 0.7–3.5 ps, depending on the species and temperature (10–16). Until now, femtosecond studies have not revealed any deviations from smoothly decaying functions in the kinetics of P*. Recently, however, complicated absorption kinetics were reported in the region of the B absorption band at room temperature (15, 16). These data were analyzed in terms of a linear reaction scheme where the state P⁺B_L⁻ is the short-lived intermediate during the transfer of the electron to H_L.

We have collected femtosecond transient spectra and kinetics in the near infrared with a high signal-to-noise ratio and high spectral and temporal resolution at cryogenic and at room temperatures. In this paper we will focus on the oscillatory features of the kinetics. We studied reaction centers of *Rhodobacter sphaeroides* R-26 and the D_{LL} mutant of *Rhodobacter capsulatus*. The latter mutant lacks the bacteriopheophytin acceptor H_L (17) and serves as a model for studying the kinetic evolution of the dimer excited state, P*, as the population of this state essentially does not decay on the time scale of a few picoseconds (18). The reaction centers of *R. sphaeroides* and *R. capsulatus* wild type display virtually similar spectral (19) and kinetic (ref. 14; J.-L.M. and J. Breton, unpublished results) characteristics, and hence the two types of reaction centers may well be compared.

MATERIALS AND METHODS

Reaction centers of the carotenoid free strain R-26 of *R. sphaeroides* were prepared as described (10). The quinone acceptor Q_A was reduced by addition of 50 mM dithiothreitol (E_m , -330 mV) to ensure complete back reaction between flashes. Preparation of chromatophores of *R. capsulatus* mutant D_{LL} that were devoid of antenna pigments is described elsewhere (20).

For cryogenic experiments, samples were diluted in glycerol ($\approx 60\%$ vol/vol) and were cooled in the dark to 100 K or to 10 K in a convection cryostat. For room temperature measurements, the sample was continuously moved perpendicular to the optical beams. The optical density of the samples was about 0.5 at 870 nm (1-mm optical path length).

Generation of the 50-fs pulses at 620 nm was essentially as described (11). The signal-to-noise ratio and the temporal resolution of the overall system were considerably enhanced by modifications in the amplification and compression chain (unpublished data). Pump pulses were centered at 870 nm and had a pulse width of either 45 fs (25-nm spectral width) or, when explicitly mentioned, 80 fs (10-nm spectral width). The

pump-probe cross-correlation (with the shorter pump pulses) was about 75 fs full width at half maximum at 800 nm. The pump and probe beams were polarized in parallel. The intensity of the pump pulses was adjusted so that 15–20% of the centers were excited upon each flash.

RESULTS

***R. capsulatus* D_{LL} Mutant.** In previous work, we studied at room temperature the excited state of the D_{LL} mutant of *R. capsulatus*, which lacks H_L, using pulses of 150 fs (18). We showed that the shape of the transient spectrum does not change in the time range of 1–100 ps and that the amplitude decays in a few hundred picoseconds. This proved that no state other than the excited state, P*, is formed in this mutant. Similar results were found at 10 K with the same experimental setup (unpublished data).

We reinvestigated the transient kinetics of this mutant at 10 K at very early times with the present setup, which gave a better signal-to-noise ratio and a better time resolution. The kinetics of the stimulated emission, as detected at 930 nm, are shown in Fig. 1. Surprisingly, the signal clearly oscillates. The amplitude of the oscillation is small (initially about 6% of the overall signal) but significant. The oscillatory part can be isolated by subtraction of a fit to a Heaviside (step) function (convoluted with the instrument response) from the experimental data. The oscillations obtained during the temporal overlap between pump and probe pulse (dotted in the oscillatory part of Fig. 1) may be due to electronic pump-probe coherence effects (21) (different from the well-known coherence artifact because the pump and probe spectra do not overlap) or fast unresolved processes, or both, and *a priori* should not be considered to reflect vibrational coherence. However, the oscillations extend far beyond this region, and hence they cannot be due to those effects. Thus, the oscillatory features reflect vibrational coherence associated with the formation of the excited state. The period of the main oscillation is about 500 fs. Three full periods are clearly visible; the signal then is damped. At first sight the signal seems to display an overall decay of a few percent in about 1 ps; more careful inspection of the oscillatory part and comparison of the data with a numerical simulation strongly suggest that a second oscillation with a period of about 2 ps

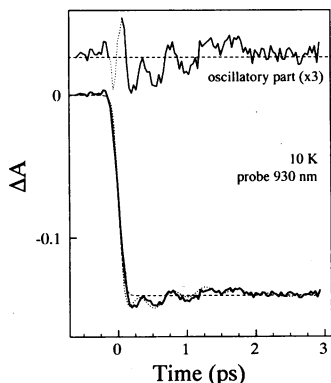


FIG. 1. Kinetics of stimulated emission at 930 nm of chromatophores of *R. capsulatus* D_{LL} at 10 K with an excitation pulse having a spectral width of 25 nm centered at 870 nm and a pulse length of 45 fs. The oscillatory part is obtained by taking the residuals of the data with a fit to a Heaviside function convoluted with the instrumental response function (dashed line). The dotted points in the oscillatory part indicate the region of pump-probe temporal overlap. The dotted line is a numerical simulation comprising the sum of a Heaviside function and two damped (time constant of 1.2 ps for both) cosines with periods of 460 fs and 2.4 ps convoluted with the instrumental response function.

is superimposed on the signal. The damping of both oscillations is similar and completed in a few picoseconds; therefore, the period of the faster oscillation is determined better than that of the slower oscillation.

We also investigated whether the oscillations are present in the Q_Y absorption region of the spectrum. Oscillations were indeed observed in the 800-nm (B band) region. Fig. 2 shows the kinetics at 812 nm, near the isosbestic point between the bleaching of the higher exciton P band [at 813 nm (18)] and the induced absorption due to P* formation (peaking at 805 nm, not shown). At this wavelength the overall signal is very weak (0.01 OD), but the modulation of the signal is relatively strong, and about six maxima are resolved. The initial period of the oscillation is ≈ 500 fs, as in the stimulated emission. The temporal separation of the peaks diminishes somewhat at later times. This might imply that different modes are involved with nearby frequencies and different damping rates. A slower oscillation with a period of about 2 ps seems to be superimposed on the faster oscillations, as in the stimulated emission. This feature is more apparent when a longer trace is considered (Fig. 2 *Inset*).

***R. sphaeroides* R-26.** It is clear that after formation of the P* state in the *R. capsulatus* D_{LL} mutant, some coherence is conserved as long as a few picoseconds. This is the time scale in which the primary charge separation in physiologically active reaction centers takes place (10–16). Therefore, we investigated whether oscillatory features could also be detected in reaction centers of *R. sphaeroides* R-26. *A priori* it may be more difficult to visualize oscillations here because (i) they are superimposed on kinetics that evolve on the same time scale and (ii) the P* state, and therewith oscillations associated only with this state, disappears in a few picoseconds.

As with the *R. capsulatus* D_{LL} mutant, oscillatory features were observed in the B-band region. However, at most wavelengths they were superimposed on the kinetics of the electrochromic shift of the B band, which reflects charge separation, and could only be visualized in the residuals of the experimental data with a fit to a monotonically evolving function. Fig. 3 shows the kinetics at 796 nm, near the isosbestic point of the band shift. Oscillations with a period of about 700 fs are clearly observed for at least two to three periods. The presence of the 700-fs oscillations in the isolated oscillatory part was independent of the assumptions made for the fit function. The mixing of the oscillations with the other kinetic features prevents the unambiguous assessment of slower oscillations; however, their presence cannot be excluded. The very fast relaxation observed at this wavelength presumably originates, apart from possible pump-probe coherence effects, from local conformational relaxations and

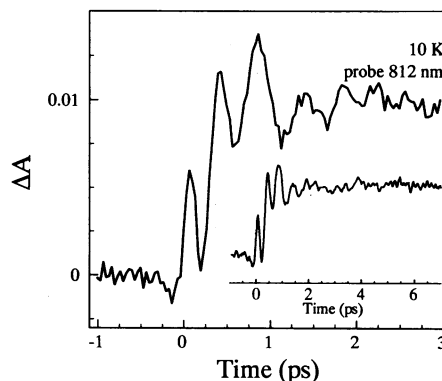


FIG. 2. Kinetics of absorption at 812 nm of chromatophores of *R. capsulatus* D_{LL} at 10 K with excitation conditions as in Fig. 1. (*Inset*) The same kinetics on a longer time scale; here the data are smoothed for better visualization of the slower (≈ 2 ps) oscillating components.

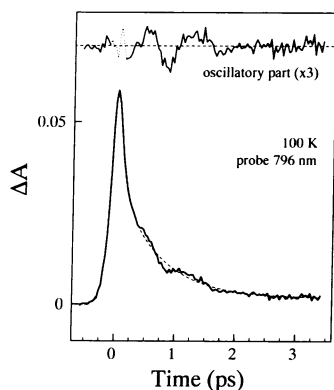


FIG. 3. Kinetics of absorption at 796 nm of reaction centers of *R. sphaeroides* R-26 at 100 K under excitation conditions as in Fig. 1. The oscillatory part is obtained by taking the residuals of the data with a fit to the sum of a δ function and an exponential decay (0.7 ps) convoluted with the instrumental response function (dashed line).

will be discussed in detail elsewhere. The data of Fig. 3 were taken at 100 K; the kinetics at 10 K are much alike except for a slightly faster attenuation of the oscillations, which we ascribe to the somewhat faster decay of P^* (12).

Fig. 4 shows the kinetics of the stimulated emission at 930 nm when excited with a broad-band pump beam (25 nm)—i.e., with the shortest pulses (of 45 fs) as in Figs. 1–3. Remarkably, under these conditions, no oscillatory features were resolved (even not in experiments with 4 ps instead of 10 ps full scale). Another unexpected result was that the kinetics needed to be fitted with a biexponential decay function [1.2 ps (80%) and 7 ps (20%) decay times]. Fits to a single exponential were unsatisfactory, as can be clearly seen in the residuals. The finding of nonmonoexponential decay was confirmed in kinetic traces of 50 ps full scale (not shown). Kinetics obtained at 10 K and at room temperature could also not be fitted with a single exponential decay function. The nonmonoexponential behavior is not due to incomplete reduction of Q_A by dithiothreitol because (i) on a millisecond time scale, all P^+ was rereduced and (ii) multiexponential decay at room temperature was also observed in samples without dithiothreitol.

It should be noted that it is due to the considerably improved signal-to-noise ratio in our data that we are now able to distinguish deviations from single exponential decay in the stimulated emission. Previous data of several groups, including our own, did not reveal any such deviations for reaction centers of *R. sphaeroides* R-26 and *R. capsulatus*

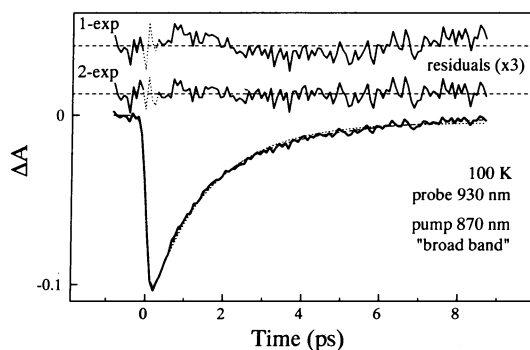


FIG. 4. Kinetics of stimulated emission at 930 nm of reaction centers of *R. sphaeroides* R-26 at 100 K under excitation conditions as in Fig. 1. Fits to a single exponential (1.5 ps) function (dotted line) and a double exponential [1.2 ps (80%) and 7 ps (20%) decay times] function (dashed line) and an asymptotic value convoluted with the instrumental response function (solid line) are shown with their residuals.

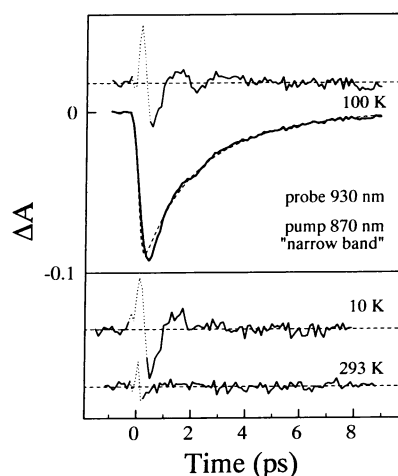


FIG. 5. Kinetics of stimulated emission (930 nm) at 100 K and oscillatory parts ($\times 3$ when normalized on the maximum signal at 100 K) at various temperatures of reaction centers of *R. sphaeroides* R-26 by using an excitation pulse of 10-nm spectral width (80-fs pulse length). The oscillatory parts are obtained by taking the residuals of the data with a fit to the sum of two exponentials and an asymptotic value convoluted with the instrumental response function (dashed line). Fit parameters at 100 K: 1.5 ps (70%) and 5.5 ps; at 10 K: 1.4 ps (85%) and 9 ps; at 293 K: 2.9 ps (65%) and 12 ps.

wild type (10–16). Heterogeneities in the kinetics of the electrochromic band shift associated with charge separation have been observed recently for reaction centers of *R. sphaeroides* R-26 (22), but these authors reported that the kinetics of the stimulated emission were single exponential.

The kinetics of the stimulated emission are significantly different upon excitation with a spectrally narrower (10 nm) pump pulse (Fig. 5). At cryogenic temperatures, a small but significant oscillation with a period of about 2 ps emerges, and, in contrast to excitation with a broad-band pump pulse, the kinetics can by no means be described by a combination of exponential decay functions. This is well-visualized when the oscillatory part is isolated. At early times they may be distorted because of pump–probe overlap effects (the pump pulse width is 80 fs instead of 45 fs in this case because of the narrower spectrum), but the modulation of the signal is obvious up to $t = 2$ ps and $t = 4$ ps at 10 K and 100 K, respectively. Again, the oscillations disappear faster at 10 K, presumably because of faster depletion of the excited state. At room temperature, no significant deviations from monotonic decay were observed.

By using a narrow excitation pulse, oscillations with a similar period and phase as that at 930 nm were observed at cryogenic temperatures at 750 nm (not shown) in the region of the broad P^* absorption band. However, these features are less well resolved than those of the stimulated emission, due to the much lower signal at this wavelength region.

The oscillating features in the kinetics at 796 nm of *R. sphaeroides* R-26 and the kinetics of the D_{LL} mutant of *R. capsulatus* were essentially the same when broad (25 nm) or narrow (10 nm) excitation pulses were used.

DISCUSSION

The data presented in this paper provide direct evidence for coherence effects in the excited state of photosynthetic reaction centers. Oscillations with a period of ≈ 400 fs to ≈ 2 ps ($15\text{--}80\text{ cm}^{-1}$) were observed under different experimental conditions. The oscillations are best observed in the D_{LL} mutant of *R. capsulatus*, which lacks the bacteriopheophytin electron acceptor H_L , because (i) the oscillations are superimposed on a stable signal and (ii) the amplitude of the

oscillations is not affected by depopulation of the excited state in the time scale of the oscillations. However, in the active reaction center, where the P^* state acts as a precursor to electron transport, vibrational coherence is also evident.

Before discussing the nature of the oscillations in some more detail, we stress the importance of the very finding that coherence is maintained for several picoseconds after formation of the excited state. This finding implies that we now have experimental evidence that vibrational relaxation does not take place on a time scale much faster than charge separation for all modes. Hence, the assumption made in the classical description of the primary electron transfer in photosynthesis that the modes which are coupled to this reaction are thermally relaxed (1, 2, 12) is not *a priori* valid. Our findings permit consideration that the primary charge separation may be a coherent rather than a stochastic process, at least at low temperature.

Further, on a phenomenological level, the presence itself of oscillations, whatever their origin, has important consequences for the collection and analysis of femtosecond kinetic data. For example, when collecting kinetics with a logarithmic sampling scheme, oscillations may be missed. Also, care has to be taken when analyzing the data in terms of a linear reaction scheme.

The observation of oscillating kinetics raises many questions regarding the nature of the modes involved, the mechanism of damping, the temperature dependence, and, last but not least, the possible coupling of these modes to electron transfer. The present limited data set does not allow an unequivocal answer to these questions. Therefore, we limit ourselves to a brief discussion of possible mechanisms involved.

The frequency range of the observed oscillations ($15\text{--}80\text{ cm}^{-1}$) is below that of the intrachromophore modes but falls within that of the protein modes (23). These modes act globally and, hence, are expected to be sensed by all chromophores. The vibrations reflected in our experiments may correspond to intradimer modes; however, such modes are presumably driven by modes of the protein matrix. It should be noted that the frequency ($\approx 120\text{ cm}^{-1}$) of a special-pair mode characterized by photochemical hole-burning (24) is significantly above the frequency range of the present oscillations.

The oscillations are clearly associated with the formation of the excited state P^* . Two main mechanisms describing their origins may be envisaged.

(i) Coherent nuclear motion within an electronic state. For instance, the absorption ($S_1 \rightarrow S_n$ transition) or the stimulated emission ($S_1 \rightarrow S_0$ transition), or both, in the excited state are modulated by the (vibrating) nuclear conformation—i.e., by the position of the wave packet (Fig. 6). Also the entire population of the excited state may be modulated in time when this state is coupled to another electronic state [e.g., a charge-separated state (dashed in Fig. 6)] because the loss of population oscillates as a result of the oscillatory arrival of wave packets in the transition zone. It should be noted that, whereas the main effect of the pump pulse will be the

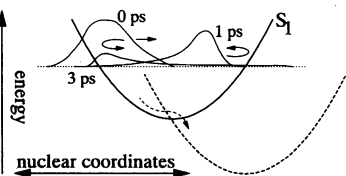


FIG. 6. Scheme of coherent motion of wave packets on the potential energy surface of the S_1 excited state. The wave packet is distorted in time because of anharmonicity and is depleted by a leak to the charge-separated state (dashed line).

(coherent) population of the excited state, in principle ground-state coherent vibrational motion can also be expected, by resonant impulsive Raman excitation (25, 26). Here, when the spectral width of the pump pulse spans a set of transitions to different vibrational levels, as is certainly the case with short pulses and low-frequency modes, ground-state vibrational levels are coherently populated by stimulated Raman emission during the pump pulse.

(ii) Electronic coherence. For the case of strong coupling between different electronic states, theoretical analysis has indicated that electronic coherence may occur (7), leading to an oscillatory component in the population of the coupled states with a frequency of twice the exchange interaction energy. So, when the coupling is in the range of $10\text{--}40\text{ cm}^{-1}$, oscillations with a period in the range of 500 fs–2 ps can be expected.

The two mechanisms are not mutually exclusive. Of course, interference between vibrational and electronic coherence and the effect of different dephasing times (7, 27) may be expressed in the kinetics. Our data will be discussed mainly in terms of the first mechanism; we have to keep in mind, however, that electronic coherence effects may also underlie the observed phenomena, notably in the case of active reaction centers.

R. capsulatus D_{LL}. In the D_{LL} mutant (Figs. 1 and 2), charge separation does not occur (18), and hence the oscillations presumably are due to modulation of the optical probe by coherent motion within the excited or ground state, or both (mechanism *i*). However, it cannot be excluded that two (or more) coupled excited states are involved. Main oscillations with periods of about 500 fs and also of about 2 ps were observed. In principle, many more vibrational modes exist in the pigment–protein complex. The fact that the two modes are seen in both stimulated emission and absorption suggests that these modes are predominantly activated upon excitation. Also, the oscillations observed in the stimulated emission are presumably due to oscillation in the excited state, as the ground state is not probed in this wavelength region. On the other hand, the kinetics at 812 nm (Fig. 2) may be complicated by ground-state oscillations, as such features are expected to be relatively strong at the wings of absorption bands (25). A much more elaborate study of the dependence of the frequencies and phases on the probe wavelength, including the lower exciton ground-state absorption band, is required to more quantitatively address these questions.

The damping of the oscillations takes place in several picoseconds in the D_{LL} mutant. Two main mechanisms of damping of the vibrational oscillations can be envisaged. First, damping may be due to vibrational dephasing, possibly accompanied by energy dissipation (vibrational relaxation). Vibrational relaxation by thermal equilibration with the protein solvent bath is indeed expected to occur in a few picoseconds (28). Second, loss of coherence by excitation of multiple normal modes having different frequencies or by anharmonicity within normal modes may play a role. The apparent increase in oscillation frequency with period number at 812 nm (Fig. 2) indicates that loss of coherence due to dispersion of frequencies probably occurs (an alternative explanation of the complicated kinetics at 812 nm may come from interference of excited-state and ground-state oscillations).

R. sphaeroides R-26. In the active reaction centers (Figs. 3–5), both vibrational and electronic coherence may in principle be reflected in the kinetics. In the absorption kinetics at 796 nm (Fig. 3), an oscillation with a period of about 700 fs is observed. This mode does not seem to act on the stimulated emission and hence does not modulate the population of P^* . This suggests that it is not directly coupled to electron transfer; it may in fact be an oscillation in the ground state. Lower frequency oscillations were not detected in the ab-

sorption kinetics around 800 nm, but these are dominated by the relatively strong signals of the electrochromic band shift.

An oscillation with a period of about 2 ps was observed in the stimulated emission. As discussed for *R. capsulatus* D_{LL}, the oscillatory features observed in the stimulated emission must reflect vibrational motion in the excited state and not in the ground state. The observation that the difference in modulation between 10 and 100 K (Fig. 5) is related to the difference in overall depletion rate supports this conclusion.

Remarkably, the oscillating feature at 930 nm could only be observed with a spectrally narrow pump pulse (Figs. 4 and 5). This behavior can be explained by an anharmonic potential energy surface of the P* state: a spectrally larger pulse excites a broader range of energies on the potential energy surface of the S₁ excited state (see Fig. 6), if it is not broader than the absorption band involved. Hence, more vibrational levels are populated, the ensemble of vibrational frequencies is more disperse, and coherence is more rapidly lost (cf. ref. 7). Alternatively, similar effects are expected if higher frequency normal modes are coherently excited by the shorter pulse.

Is Charge Separation Coupled to Low-Frequency Modes? A key question is, of course, whether the 2-ps oscillation is coupled to the electron-transfer reaction. We have no direct evidence for such a coupling. Evidence could come from probing the unfortunately very weak bacteriochlorophyll cation and bacteriopheophytin anion bands. However, the observation of the ≈2-ps oscillations at 930 nm and at 750 nm is consistent with a mechanism of coherent electron transport.

If the charge separation reaction would be coupled to a mode of ≈2 ps, this would have some very interesting consequences as follows.

(i) In contrast to the conventional electron-transfer picture, such a reaction would be nearly adiabatic—i.e., the probability of charge separation upon passage of the transition zone is near unity.

(ii) By using the collective character of low-frequency protein vibrational modes, the charge transfer process may be visualized as a charge distribution, oscillating over the pigment-protein complex, including the accessory bacteriochlorophylls. Such effect might explain observations leading to the proposal of P⁺B_L⁻ as intermediate state (15, 16). A somewhat different situation has been described in a theory of coherent electron transport in which the state P⁺B_L⁻ is included as a separate state (4, 5).

(iii) A coherent and adiabatic mechanism of the primary charge separation would shine a new light on the origin of the weak temperature dependence of this reaction. Until now, efforts to model this feature have only been made by assuming that the reaction is nonadiabatic and coupled to thermally equilibrated modes (2, 3, 12).

Altogether, it seems reasonable to propose that coherence plays an important role in the ultrafast and highly efficient primary charge-separation process. The combination of the extremely high rate of the forward reaction and the low rate of the back reaction may well be related to loss of coherence, possibly associated with dissipation of vibrational energy, upon formation of the charge-separated state.

Part of this work has been supported by grants from Institut National de la Santé et de la Recherche Scientifique and Ecole Nationale Supérieure de Techniques Avancées. D.C.Y. was supported by Department of Energy Grant DE/FG02/90ER and National Institutes of Health Grant R1GM42645A. M.H.V. is recipient of a grant from the Science Program of the European Economic Community.

- Marcus, R. A. & Sutin, N. (1985) *Biochim. Biophys. Acta* **811**, 265–322.
- Bixon, M. & Jortner, J. (1986) *J. Chem. Phys.* **90**, 3795–3800.
- Bixon, M. & Jortner, J. (1982) *Faraday Discuss. Chem. Soc.* **74**, 17–29.
- Marcus, R. A. & Almeida, R. (1990) *J. Phys. Chem.* **94**, 2973–2977.
- Almeida, R. & Marcus, R. A. (1990) *J. Phys. Chem.* **94**, 2978–2985.
- Joseph, J. S., Bruno, W. & Bialek, W. (1991) *Biophys. J.* **59**, 30 (abstr.).
- Jean, J., Friesner, R. A. & Fleming, G. R. (1991) *Ber. Bunsenges. Phys. Chem.* **95**, 253–258.
- Allen, J. P. & Feher, G. (1984) *Proc. Natl. Acad. Sci. USA* **81**, 4795–4799.
- Deisenhofer, J. P., Epp, O., Miki, K., Huber, R. & Michel, H. (1984) *J. Mol. Biol.* **180**, 385–398.
- Martin, J.-L., Breton, J., Hoff, A. J., Migus, A. & Antonetti, A. (1986) *Proc. Natl. Acad. Sci. USA* **83**, 957–961.
- Breton, J., Martin, J.-L., Fleming, G. R. & Lambry, J.-C. (1988) *Biochemistry* **27**, 8267–8284.
- Fleming, G. R., Martin, J.-L. & Breton, J. (1988) *Nature (London)* **333**, 190–192.
- Woodbury, N. W., Becker, M., Middendorf, D. & Parson, W. W. (1985) *Biochemistry* **24**, 7516–7521.
- Kirmaier, C. & Holten, D. (1988) *FEBS Lett.* **239**, 211–218.
- Holzappel, W., Finkle, U., Kaiser, W., Oesterheld, D., Scheer, H., Stolz, H. U. & Zinth, W. (1989) *Chem. Phys. Lett.* **160**, 1–7.
- Holzappel, W., Finkle, U., Kaiser, W., Oesterheld, D., Scheer, H., Stolz, H. U. & Zinth, W. (1990) *Proc. Natl. Acad. Sci. USA* **87**, 5168–5172.
- Robles, S. J., Breton, J. & Youvan, D. C. (1990) *Science* **248**, 1402–1405.
- Breton, J., Martin, J.-L., Lambry, J.-C., Robles, S. J. & Youvan, D. C. (1990) in *Reaction Centers of Photosynthetic Bacteria*, ed. Michel-Beyerle, M.-E. (Springer, Berlin), pp. 293–302.
- Breton, J., Bylina, E. J. & Youvan, D. C. (1989) *Biochemistry* **28**, 6423–6430.
- Robles, S. J., Breton, J. & Youvan, D. C. (1990) in *Reaction Centers of Photosynthetic Bacteria*, ed. Michel-Beyerle, M.-E. (Springer, Berlin), pp. 283–291.
- Pollard, W. T., Brito Cruz, C. H., Shank, C. V. & Mathies, R. A. (1989) *J. Chem. Phys.* **90**, 199–208.
- Kirmaier, C. & Holten, D. (1990) *Proc. Natl. Acad. Sci. USA* **87**, 3552–3556.
- Gö, N., Noguti, T. & Nishikawa, T. (1983) *Proc. Natl. Acad. Sci. USA* **80**, 3696–3700.
- Johnson, S. G., Tang, D., Jankowiak, R., Hayes, J. M., Small, G. J. & Tiede, D. M. (1990) *J. Phys. Chem.* **94**, 5849–5855.
- Chesnoy, J. & Mokhtari, A. (1988) *Phys. Rev. A* **38**, 3566–3576.
- Yan, Y. X. & Nelson, K. A. (1987) *J. Chem. Phys.* **87**, 6240–6265.
- Onuchic, J. N. & Wolynes, P. G. (1988) *J. Phys. Chem.* **92**, 6495–6503.
- Doany, F. E., Greene, B. I. & Hochstrasser, R. M. (1980) *Chem. Phys. Lett.* **75**, 206–208.